Blending of *Moringa oleifera* into Biodegradable Polycaprolactone/Silver Electrospun Membrane for Hemocompatibility Improvement

Madeeha Sadia[1,2] · Muhammad Aiman Mohd Zaki[1] · Saravana Kumar Jaganathan[3] ·
Muhammad Faiz Md Shakhih[1] · Aisyah Salihah Kamarozaman[4] · NorulNazilah Ab'lah[4] · Syafiqah Saidin[1,5]

Abstract

Moringa oleifera (*M. oleifera*) has been utilized in conventional drug to treat illnesses associated with inflammation and wound healing. However, its utilization in tissue engineering application has not been explored yet. Reliable materials and carrier system are required to blend *M. oleifera* for sustainable therapeutic purpose. In this study, *M. oleifera* leave extracts were incorporated into electrospun polycaprolactone (PCL) nanofibrous membrane at various concentrations (19 wt%, 39 wt% and 59 wt%). A standard composition of 1 wt% silver nanoparticles (AgNPs) was also included to improve the membrane performance. The membranes were characterized with SEM–EDX, AFM and ATR-FTIR analyses. Further performances on the wettability, thermal, antibacterial and biocompatibility of the membranes were detailed assessed. The PCL/*M. oleifera*/AgNPs (PMA) membranes were viewed with smaller nanofiber diameter, greater surface roughness and higher wettability following the incorporation of *M. oleifera*. The notable appearances of C=C and N–O functional groups were observed on the PMA membranes with the composition of less than 1 wt% Ag. The PMA membranes were clarified thermally stable with a single step thermal decomposition. The antibacterial efficacy of the PMA membranes was prominent on *Staphylococcus aureus* (*S. aureus*) than *Escherichia coli (E. coli)*. Importantly, the PMA membranes have enhanced the human platelet coagulant behavior significantly ($p \leq 0.05$), up to 39% for the PMA-3. The membranes are considered hemocompatible with a hemolysis index of $\leq 5\%$. These results demonstrate that the PMA electrospun membranes have a potential to be used in tissue engineering application due to the therapeutic properties of *M. oleifera*.

✉ Syafiqah Saidin
  syafiqahsaidin@biomedical.utm.my;
  syafiqahsaidin@gmail.com

1   Department of Biomedical Engineering and Health Sciences, Faculty of Electrical Engineering, Universiti Teknologi Malaysia, 81310 Johor Bahru, Johor, Malaysia

2   Department of Biomedical Engineering, Faculty of Electrical and Computer Engineering, NED University of Engineering and Technology, Karachi, Pakistan

3   School of Engineering, College of Science, University of Lincoln, Brayford Pool, Lincoln LN6 7TS, UK

4   Centre of Foundation Studies, Universiti Teknologi MARA, Cawangan Selangor, Kampus Dengkil, 43800 Dengkil, Selangor, Malaysia

5   IJN-UTM Cardiovascular Engineering Centre, Institute of Human Centered Engineering, Universiti Teknologi Malaysia, 81310 Johor Bahru, Johor, Malaysia

1 Introduction

Wounds are easily being infected, that will delay/disrupt the tissue healing process [1]. Delay in wound healing and prominent contamination could lead to tissue necrosis and ultimately cause mortality [2]. More than 40 million people worldwide suffer from wound diseases where the treatment cost is estimated to reach $15 billion annually [3]. In fact, since the late 1990s, there have been considerably more data recorded on the expansion of worldwide wound care industries [3]. In this scenario, effective treatment options to speed up the healing phases are necessary to be explored [3]. Over the centuries, traditional herbal products based on plant extracts have been practiced in many countries to enhance wound healing and in the search for novel pharmaceuticals that have therapeutic capabilities [4]. The application of plant

extracts, as well as other alternative forms of medical therapy, has recently been merged with modern technology. As a result, several investigations have been conducted to find and combine materials/technique that are suitable for wound healing application [5].

Medicinal plant extracts are well recognized for their capacity to nourish wound lesion with their healing, antibacterial, anti-inflammatory, analgesic and tissue regeneration abilities [6]. *Moringa oleifera* (*M. oleifera*) has been proven to have a variety of therapeutic qualities, which are linked to its phytochemicals of flavonoids, tannins, alkaloids and steroids [7]. The aqueous and ethanolic *M. oleifera* leave extracts have shown good potential to mediate wound healing [8]. In recent reviewed article, Mahato et al. [9] also reported the antibacterial activity of *M. oleifera* against Gram-positive and Gram-negative bacteria. Therefore, it is beneficial to blended *M. oleifera* leaves extract into a carrier system to be used in wound healing application.

The selection of wound healing carrier system is relied on the system capability to store and release drugs/herbs. Commonly, biodegradable materials such as polymer are being used as the carrier system. Polycaprolactone is a semi-crystalline, aliphatic and thermoplastic polymer which comprised of ester groups that are responsible for its biodegradability [10]. It has been widely employed in tissue engineering applications such as bone replacement, wound dressing, vascular tissue engineering, nerve repair, etc. [11]. Recently, researchers have shown intense interest in PCL synthetic polymer due to its appealing features of biocompatibility, appropriate mechanical strength and biodegradability where PCL is also a good option to accommodate drugs/plants in its designed scaffolds for wound treatment application [11]. However, the incorporation of high composition of drugs/plants into the polymeric matrices of PCL will alter the polymer's genuine properties, thus erupting its performances. Therefore, continuous characterizations and assessments should be performed following the blending of drugs/plants into the PCL.

Electrospinning is one of the fabrication techniques, commonly used to develop PCL membrane, owing to its ease of usage and its capability to retain polymeric properties [12]. Tissue membranes made of electrospun polymers have recently piqued researcher's interest due to its scaffolding design, which mimic skin properties for nutrition penetration, gas exchange, waste excretion, porous structure and large specific surface area [13]. Although numerous studies in recent years have explored on the development of electrospun biomaterials, the utilization of materials for the acceleration of tissue healing and the rapid prevention of bacterial infection is still under huge demand. As a result, the quests for an appropriate membrane substitute-based biomaterials continue to be the point gap in tissue engineering [14].

Previously, it was reported that with the use of different filler elements, such as nanoparticles, has improved the overall performance of biomaterials, significantly [15]. Silver nanoparticles (AgNPs) have been widely researched as an antibacterial agent against a wide range of pathogenic bacteria such as *Escherichia coli* (*E. coli*), *Staphylococcus aureus* (*S. aureus*), *Staphylococcus epidermidis* (*S. epidermidis*), *Staphylococcus haemolyticus* (*S. haemolyticus*) and *Pseudomonas aeruginosa* (*P. aeruginosa*) [16]. However, the ease of Ag dissolution limits the efficacy of AgNPs in actual applications. As a result, AgNPs have been combined with biodegradable polymers to retain its stability and antibacterial activity [17]. Although AgNPs have positive outcomes to treat infection but at higher consumption, toxicity is the main issue [18]. Besides, AgNPs are more prominent to kill Gram-negative bacteria than Gram-positive bacteria. Saidin et al. [16] also mentioned that organic material such as *M. oleifera* would be more effective to kill Gram-positive bacteria. Therefore, it is an ideal approach to blend AgNPs and *M. oleifera* to provide strong antibacterial synergistic effects, covering a wide spectrum of Gram-negative and Gram-positive bacteria.

The aim of this study was to blend various concentrations of *M. oleifera* and a standard low concentration of AgNPs into PCL electrospun membranes for wound healing system. The electrospun membranes were evaluated through physicochemical characterization analyses of scanning electron microscopy equipped with energy dispersive X-ray (SEM–EDX), atomic force microscopy (AFM) and attenuated total reflection-Fourier transform infrared spectroscopy (ATR-FTIR). The wettability and thermal properties of the membranes were investigated through contact angle and thermogravimetric (TGA) analyses, respectively, while the capability of the membranes to retard *E. coli* and *S. aureus* growth was clarified through *in vitro* antibacterial analyses of zone inhibition, bacterial count test and live/dead staining. The platelet coagulant and hemocompatibility of the electrospun membranes were finally proved with human blood.

2 Materials and Methods

2.1 Membrane Preparation

2.1.1 Preparation of *M. oleifera* Extract

The fresh leaves of *M. oleifera* were purchased from the local market of Johor Bahru, Malaysia. The plant species were verified at the Forest Biodiversity—Forest Research Institute Malaysia (FRIM), with a voucher number of FSG9. The leaves were thoroughly cleaned and dried in an oven (UFE800, Memmert Universal Oven, Germany) at 60 °C for 72 h. Then, the dried leaves were ground into fine powders

using mortar and pestle. An amount of 5 g crumbled dried leaves was immersed in 100 mL of pure methanol solution (Merck, Germany) and agitated continuously for 72 h. A Whatman No. 1 filter paper was used to filter the extract solution. The resulting dark green filtrate solution was then evaporated to remove the solvent, followed by an air evaporation method using a fume hood for the duration of 48 h. The prepared *M. oleifera* leaves extract was kept in a refrigerator at 4 °C for further use.

2.1.2 Preparation of Electrospinning Solution

The PCL solution (80,000 Mw, Sigma-Aldrich, Germany) was prepared by mixing 15 wt% PCL beads in a combination solvent of chloroform (Merck, Germany) and methanol (8:2 v/v). The PCL solution was stirred for 1 h at 300 rpm, under normal room temperature. Polycaprolactone/*M. oleifera*/AgNPs electrospinning solutions were designed by incorporating different concentrations of *M. oleifera* leaves extract (19%, 39% and 59%) and 1 wt% AgNPs (< 100 nm, Sigma-Aldrich, Germany) into the PCL solution. Each electrospinning solution was mixed and agitated for 1 h.

2.1.3 Electrospinning Process

The electrospinning solution was administered into 10 mL standard syringe, attached with 21G blunted stainless steel needle. The syringe was positioned on a syringe pump (SP-1000, N-Fiber, USA) and set at a flow rate of 1 mL/h. The electrospinning solution was pulled out into nanofibers at a distance of 15 cm with a high voltage of 10 kV (Gamma High Voltage Research Inc, FL, USA). In this study, the following proposed formulations of electrospun membranes were studied and represented as PCL (100% PCL), PMA-1 (80% PCL/19% *M. oleifera*/1% AgNPs), PMA-2 (60% PCL/39% *M. oleifera*/1% AgNPs) and PMA-3 (40% PCL/59% *M. oleifera*/1% AgNPs).

2.2 Characterization Analyses

The PCL and PMA electrospun membranes were platinum-coated prior the morphology and atomic percentage analyses using SEM instrument (Hitachi Tabletop Microscope, TM3000, Japan) coupled with energy dispersive X-ray (EDX) system. Mean fiber diameter and membrane pore size were calculated based on the SEM images using Image J software (Java 1.4, National Institute of Mental Health, USA). A digital micrometer gauge (Mitutoyo, 293-240-30, Japan) was used to measure the membrane thickness. By cutting the membranes into 10 mm × 12 mm rectangular shape, Eq. 1

was used to calculate the membrane porosity:

$$Porosity(\%) = \frac{Apparent\ Density\left(\frac{g}{cm^3}\right)}{Bulk\ density\left(\frac{g}{cm^3}\right)} \tag{1}$$

The average roughness (R_q) of each membrane was identified using AFM instrument (Hitachi, AFM 5000 II, Japan) to capture the topography of the electrospun membranes under a tapping mode on the area of $10 \times 10 \ \mu m^2$ by implementing 1.50 Hz oscillation frequency through AFM 5000 II software (II, Hitachi, Japan) at three different areas. The chemical functionalities of the electrospun membranes were then analyzed using ATR-FTIR unit (Shimadzu's, IR Tracer 100, Japan). The ATR-FTIR spectra were collected within 600–4000 cm^{-1} wavenumber at 4 cm^{-1} resolution and 32 average scans.

The wettability characteristics were also measured using a contact angle measurement unit (Ast products. Inc, VCA Optima, USA) with distilled water droplet size of 1 μL at room temperature. The water was dropped on three different membrane surface areas to obtain the average wettability records. The thermal stability of the electrospun membranes was analyzed using TGA instrument (TA-Q500, TA instruments, USA) to assess the thermal decomposition of the electrospun membranes at different temperatures. The test was carried out in a nitrogen atmosphere where the membranes were heated at a rate of 10 °C/min between the temperatures of 30 °C and 1000 °C.

2.3 In-Vitro Antibacterial Test

Two significant quantitative schemes (zone inhibition and bacterial count) and one qualitative scheme (live/dead) were used to investigate the antibacterial behavior of the PCL and PMA membranes. Another two electrospun membranes composed of PCL/AgNPs (PA) and PCL/*M. oleifera* (PM) were fabricated and added to the antibacterial analysis for the identification of single antibacterial effect. All analyses were conducted on Gram-negative *E. coli* (ATCC 11229) and Gram-positive *S. aureus* (ATCC 6538) bacterial strains in triplicate measurement.

All apparatus and reagents were initially sterilized in an autoclave (HVE-50, Hirayama, Japan) at 120 °C for 30 min prior to the antibacterial tests. The pure cultures of bacteria from the bacterial cryopreserved stocks were streaked on Luria–Bertani (LB) nutrient agar plates and incubated at 37 °C for 24 h. Later, a single colony of each bacterium was inoculated into 100 mL of LB broth using a sterile inoculation loop. The cultures were agitated for 16 h at 180 rpm in a shaking incubator (SI-50D, Lab-Tech Scientific, Malaysia). Using ultraviolet–visible (UV–Vis) spectrophotometer (GENESYS 10S, Thermo Scientific, USA), the

optical density of the bacterial suspension was examined and adjusted to 1×10^6 cells/mL at 600 nm wavelength for further use, while the electrospun membranes were punched into 12 mm diameter circular shape with a customized punch tool. Prior to all antibacterial tests, the circular shaped electrospun membranes were sterilized for 15 min on each side using the UV light.

2.3.1 Zone Inhibition

The first quantitative zone inhibition test was conducted to determine the ability of the electrospun membranes to retard bacterial growth by diffusing its antibacterial agent toward the environment. Sterile cotton sticks were plunged into the bacterial suspensions of 1×10^6 cells/mL *E. coli* and *S. aureus*, independently, and spread homogenously on new LB agar plates. The sterilized electrospun membranes were then placed firmly on the LB nutrient agars which have been smeared with the bacteria. The agar plates were incubated for 24 h at 37 °C. The inhibition zones were then measured on the clear zones around the membranes.

2.3.2 Bacterial Count Test

The second quantitative bacterial count percentage test was conducted by immersing the sterilized electrospun membranes in 5 mL of bacterial solution that contained 1×10^6 cells/mL bacteria. These bacterial suspensions were then incubated for 3 h at 180 rpm in a shaking incubator. After the 3 h incubation, the membranes were removed and the bacterial suspensions were diluted till six folds. A drop plate method was used to grow the treated bacteria by dropping the dilution series of 10 µL onto new LB nutrient agars. The agar plates were incubated at 37 °C for 24 h. The colony forming units (CFU) were then determined by manually counting bacterial colonies that formed on the LB agars. The reduction percentages (bactericidal) were finally calculated by using Eq. 2:

$$\text{Bactericidal reduction}\,(\%) = \frac{\text{CFU}_{(\text{control})} - \text{CFU}_{(\text{experiment})}}{\text{CFU}_{(\text{control})}} \times 100$$

(2)

2.3.3 Live/Dead Staining

For the qualitative assessment, the bacterial suspensions from the 3 h incubation were centrifuged for 15 min at 10,000 rpm. The isolated bacterial pellets were re-suspended in 20 mL of 0.85% sodium chloride (NaCl). The solutions were gently shaken every 15 min for 1 h period for the washing process. The solutions were then centrifuged again for 15 min at

10,000 rpm. The final pellets were collected and added with 1 mL of NaCl solution. The final re-suspended bacteria were stained with the LIVE/DEAD Bacterial Viability Kit L13152 (Invitrogen, USA). A fluorescent inverted microscope (Axio Vert A1, Carl Zeiss, Germany) was used to observe the live/dead bacteria at $40 \times$ magnification in dark environment. The SYTO 9, a green nucleic acid stain, marked all bacteria in the population, including those with intact and damaged membranes, while the propidium iodide, a red nucleic acid stain, passed through the broken bacterial membrane and replaced the SYTO 9 [19]. As a result, in the fluorescent images, active bacteria were colored green and dead bacteria were stained red.

2.4 In-Vitro Cell Test

The coagulant ability and hemocompatibility of the electrospun membranes were clarified with human blood through coagulant prothrombin time (PT) and hemolysis assays, respectively [20]. Both tests were performed following the approval by the National Heart Institute (IJN), Kuala Lumpur, Malaysia with a ref no: IJNREC/364/2018 in triplicate.

2.4.1 Prothrombin Time Assay

The human blood was collected with consent from healthy individuals through a venipuncture method and stored in sodium citrate blood tubes. In retrieving platelet-poor plasma (PPP), the blood was centrifuged at 3000 rpm for 10 min at room temperature. The coagulant activity of electrospun membranes was determined using PT assay to determine the capability of the membranes to coagulate blood through extrinsic pathway. The PT assay procedures were started by washing the electrospun membranes with deionized water; then, the membranes were incubated in PBS for 30 min at 37 °C. The membranes were mixed with 50 µL of PPP and carefully stirred with a sterile steel needle for 1 min at 37 °C, followed by the addition of 50 µL of NaCl-thromboplastin reagent (Factor III). The mixtures were gently shaken until the observation of clot formation. The time taken for the formation of clot was recorded as PT.

2.4.2 Hemolysis Assay

The electrospun membranes (5 mm $\times$ 5 mm) were submerged into 0.9% (w/v) PBS for 30 min at 37 °C and dipped separately for 1 h at 37 °C in prepared aliquots containing a solution of citrated blood and PBS at a ratio of 4:5. The immersed membranes were delicately removed, and all exposed solutions were centrifuged at 3000 rpm for 10 min. Finally, the optical density (OD) of the supernatant was observed using a spectrophotometer (GENSYS 10S UV–Vis,

Thermo Scientific, US) at 542 nm. Under the same condition, a blend of blood and PBS was denoted as the positive control (PC: 0% hemolysis), while the blood with PBS was denoted as the negative control (NC: 100% hemolysis). Equation 3 was used to calculate the hemolytic action (γ):

$$\gamma = \frac{OD_t - OD_{PC}}{OD_{NC} - OD_{PC}} \times 100\% \tag{3}$$

2.5 Statistical Analysis

All quantitative data were collected in triplicate and presented as mean $\pm$ standard deviation (SD). The antibacterial efficacies were evaluated using Analysis of Variance (ANOVA) statistical analysis, followed by post hoc Dunnett's test at $p \le 0.05$. For the blood compatibility data, the statistical measurement was done using ANOVA followed by post hoc Tukey's test at $p \le 0.05$.

3 Results and Discussion

3.1 SEM–EDX Analysis

The SEM images in Fig. 1a show the morphology of pristine PCL and PMA membranes. All electrospun membranes retained the homogenous, continuous, tangled and bead-free nanofibers morphology. Disperse aggregates were observed on the PMA membranes which demonstrated the incorporation of AgNPs into the combination matrix of PCL and *M. oleifera* leaves extract. In this study, Image J software was used to measure the average diameter of the nanofibers by randomly selecting 60 electrospun nanofibers. Decrease in the average fiber diameter was observed in comparison with the pristine PCL membranes as listed in Table 1. Similar observation was also reported in the previous literature on the fabrication of PCL/*Clerodendrum phlomidis* electrospun membranes [21]. However, as the amount of *M. oleifera* concentration increased, there was a little increment in the fiber diameter due to less PCL concentration and more extract quantity that directed to the swelling of nanofibers at the highest concentration of *M. oleifera* (PMA-3).

Porosity was identified as a critical criterion for assessing the efficacy of fibrous materials for tissue engineering scaffolds [4]. Adequate porosity enables oxygen to permeate and diffuse from the air to the wound, which is an excellent approach to speed up tissue healing [2]. In this study, the PMA electrospun membranes exhibited the reduction in fiber diameter than the pristine PCL which favored the reduction in pore size. All PMA electrospun membranes showed a porous structure with more than 75% porosity (Table 1) which is beneficial for cell adhesion and proliferation [4].

The results also revealed that the porosity of the electrospun membranes increased in the presence of *M. oleifera* leaves extracts. However, at the blending of 59% *M. oleifera* leaves extract (PMA-3), the porosity percentage declined to 78.86% from 85.40% (PMA-2) which is associated with the swelling of nanofibers that increased the surface area and reduced the apparent density of the membranes.

The elemental composition of the electrospun membranes was analyzed through EDX analysis as displayed in Fig. 1b. All electrospun membranes were mainly composed of carbon (C) and oxygen (O) elements. The peaks of aluminum (Al) were annotated due to the use of aluminum foil sheet as the platform collector. The incorporation of AgNPs in the PMA-1, PMA-2 and PMA-3 causes the appearance of additional new peak, between 2.2 and 2.5 keV, which was assigned to Ag element/compound. The blending of AgNPs into the PCL/*M. oleifera* solution that contained chloroform and methanol as the material solvent initiated the reaction between Ag and Cl from the chloroform to form AgCl. Thus, the detection of Ag element/compound was shifted to 2.2–2.5 keV instead of the prominent Ag peak at 3.0 keV. Sun et al. [22] noticed the detection of Ag/AgCl between 2.5 and 3.0 keV when the Ag/AgCl was combined with the Ag nanowires. However, in this study, Cl element was not directly observed in the EDX spectra for all electrospun membranes due to the evaporation of excessive chloroform. The changes in the concentration of PCL and *M. oleifera* extracts have produced inconsistency on the Ag atomic percentages in accordance with the visualization of Ag aggregates on the SEM images.

3.2 AFM Analysis

The topographies and surface roughness of the PCL and PMA electrospun membranes were recorded by AFM as shown in Fig. 1c. The PCL membranes have the lowest surface roughness in root mean square (R_q) value, which further increased by adding the fixed amount of AgNPs and different quantities of *M. oleifera* leaves extract. The dispersion of Ag in the form of agglomerates and the incorporation of *M. oleifera* leaves extract within the PCL membranes have changed the interaction between the PCL assembly [23] that resulted in the appearance of more separate aggregation in the form of hill and valley topographies, thus increasing the surface roughness. These rough surfaces are forecasted to favor cells adhesion and proliferation [23].

3.3 ATR-FTIR Analysis

Figure 2 shows the ATR-FTIR spectra of electrospun PCL, PMA-1, PMA-2 and PMA-3 electrospun membranes. The PCL membranes were annotated with –CH^2 (symmetric and asymmetric) vibrations between 2939 and 2864 cm^{-1}, C=O stretching vibrations of the ester group at 1722 cm^{-1}, CH_2
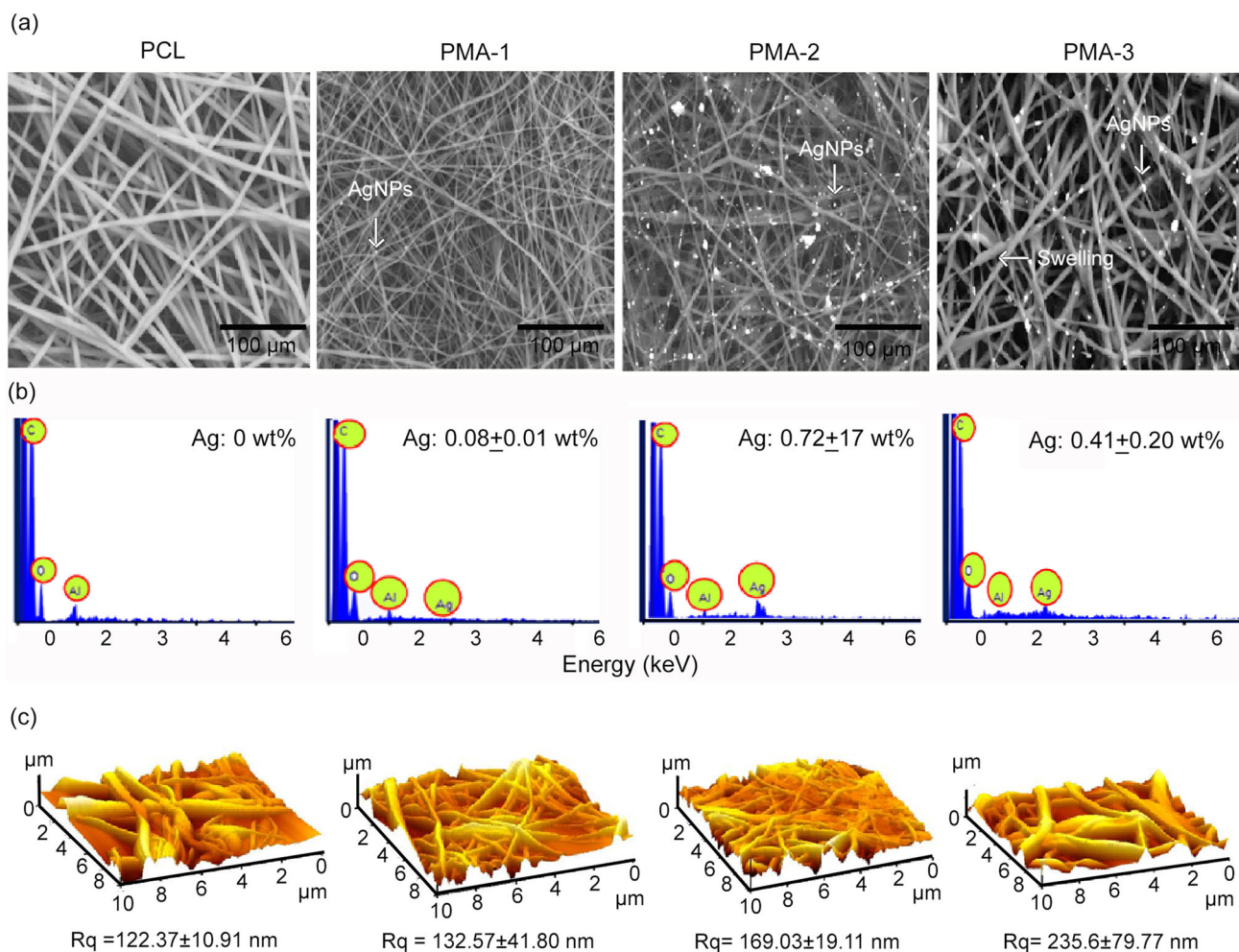
Fig. 1 **a** SEM images, **b** EDX spectra and **c** AFM topography images of electrospun PCL, PMA-1, PMA-2 and PMA-3 nanofibrous membranes

Table 1 Average fiber diameter, pore size and porosity of electrospun nanofiber

Formulation	Sample	Average diameter (μm)	Pore size (μm)	Porosity (%)
PCL-100%	PCL	2.13 ± 0.45	5.38 ± 2.28	74.59
PCL80%/*M. oleifera*19%/AgNPs1%	PMA-1	0.99 ± 0.41	1.88 ± 0.58	80.00
PCL60%/*M. oleifera*39%/AgNPs1%	PMA-2	1.07 ± 0.34	1.39 ± 0.44	85.40
PCL40%/*M. oleifera*59%/AgNPs1%	PMA-3	1.77 ± 0.49	3.01 ± 1.09	78.86

bending vibrations at 1366–1418 cm^{-1} and C–O–C stretching vibrations at 1045, 1165 and 1238 cm^{-1}. The PMA membranes showed the appearance of similar PCL-related stretching modes, but at lower peak intensities.

The PMA-2 spectrum has slight broad new peaks between 3195 and 3595 cm^{-1}, indicating the presence O–H stretch, N–H stretch vibrations, related to alkynes, carboxylic acids, primary and secondary amines as well as amides [24]. As the amount of *M. oleifera* leaves extract increased, the PMA-2 has displayed the fingerprint of one new small peak raised

between 1550 and 1680 cm^{-1} which mediated the compositions of C=C stretch (aromatics) and N–O of *M. oleifera*. The PMA-3 at the highest *M. oleifera* leaves extract concentration further increased the peak shifting at 3100–3675 cm^{-1} with more existences of C–H stretch (alkenes and aromatics) functional groups. On the fingerprint area, the spectrum displayed obvious C=C and N–O peaks.
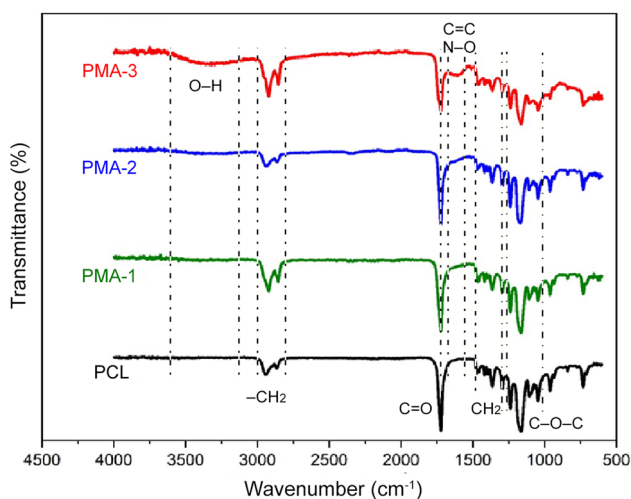
Fig. 2 ATR-FTIR spectra of electrospun PCL, PMA-1, PMA-2 and PMA-3 electrospun membranes

3.4 Wettability Analysis

The wettability of electrospun membranes was investigated to evaluate the influence of AgNPs and *M. oleifera* leaves extracts on the hydrophobicity of pure PCL membranes. Water droplets were used to determine the contact angle on the pristine PCL, PMA-1, PMA-2 and PMA-3 electrospun membranes after 10 s of droplet exposure. The contact angles for the PCL, PMA-1, PMA-2 and PMA-3 were average calculated to be $126.57 \pm 2.00°$, $18.00 \pm 3.65°$, $19.30 \pm 2.40°$ and $8.73 \pm 0.42°$, respectively. It was notified that the rise in hydrophilicity of the pristine PCL membranes was due to the existence of *M. oleifera* leaves extract within the PCL matrices as the Ag amount was fixed during the fabrication of PMA membranes. The existence of polar phytochemicals and the availability of multiple hydrophilic –OH groups [25] in the *M. oleifera* chemical structure have contributed to the hydrophilicity of the PMA membranes.

3.5 TGA Analysis

The TGA was used to determine the thermal behavior or thermal stability of the electrospun membranes. The weight loss of the electrospun membranes was recorded between the temperature of 0 °C and 1000 °C. The recorded TGA curves are plotted in Fig. 3a, and the summarized TGA results are shown in Table 2. The PMA electrospun membranes showed gradual reduction on the initial onset degradation temperature and gradual reduction on the ranges of quasistatic temperature, compared to the pristine PCL. The variation percentages of weight decomposition were also reduced from 99.96 to 84.24% when the electrospun membranes were blended with the standard AgNPs amount and the highest *M. oleifera*
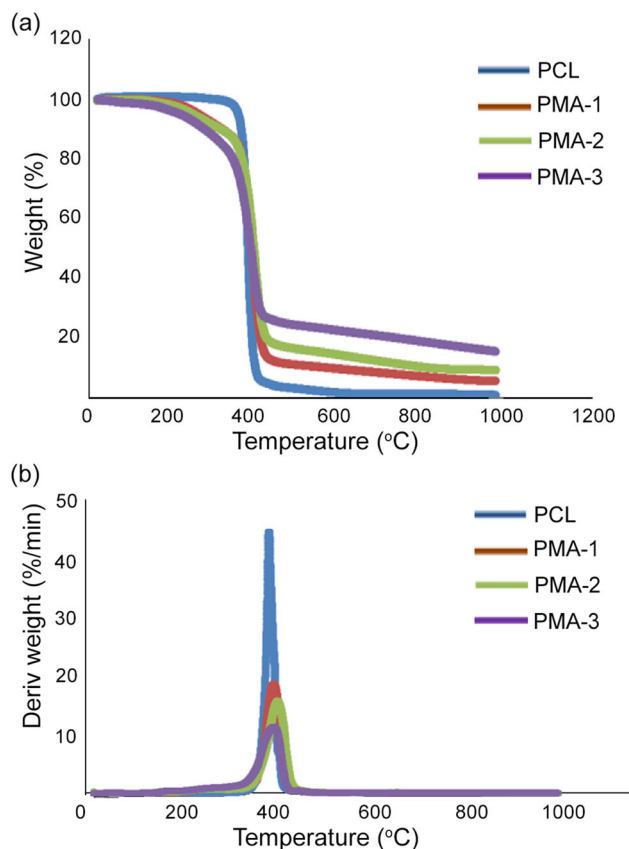

Fig. 3 a TGA and **b** DTG curves of electrospun PCL, PMA-1, PMA-2 and PMA-3 electrospun membranes

leaves extract concentration. Furthermore, the PMA electrospun membranes showed increment of weight residues compared to the PCL membranes.

These results indicate that the PCL matrix was blended well with *M. oleifera* leaves extract and AgNPs [23] where both fillers reduced the polymer entanglement, cause the chemical bonds of the polymer easier to be decomposed [21]. Water evaporation also contributed to the thermal degradation behavior as *M. oleifera* leaves extract has higher water content compared to the PCL. However, the presence of crosslinking bonds and aromatic structure of *M. oleifera* leaves extract led to difficulties in decomposing the total weight membranes, thus producing greater residues and higher T_{max} as shown in Fig. 3b. The DTG curves in Fig. 3b also demonstrate that all membranes were thermal degraded with a single step thermal decomposition.

3.6 Antibacterial Efficacy

3.6.1 Zone Inhibition Analysis

The measurements of zone inhibition in Fig. 4a show that the PMA electrospun membranes have both Gram-negative
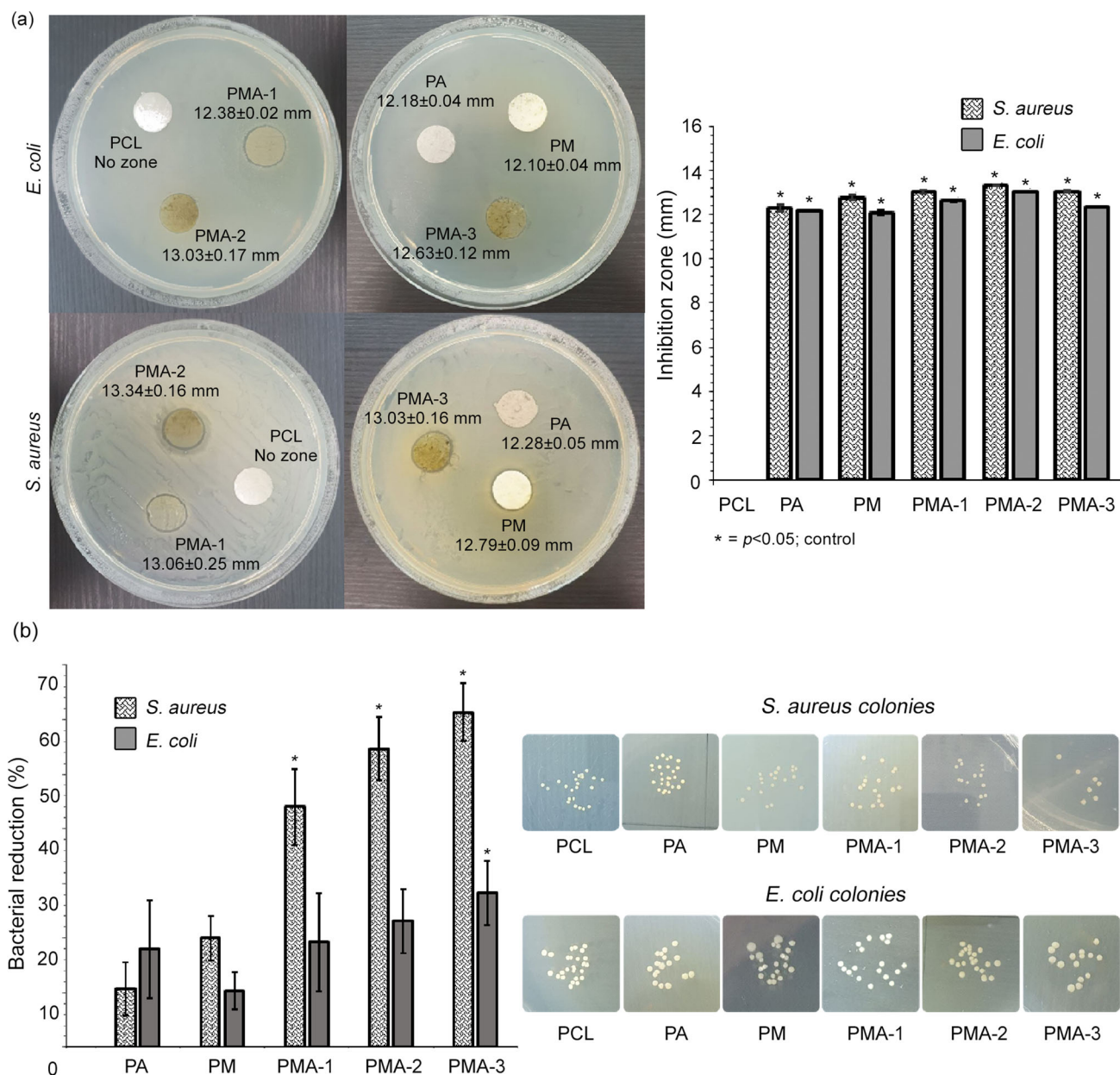
Fig. 4 a Inhibition zones and **b** bacterial reduction data analyses on electrospun PCL, PMA-1, PMA-2 and PMA-3 electrospun membranes after 24 h incubation

E. coli and Gram-positive *S. aureus* bactericidal ability which prosperous to be employed in wound infection treatment. The raising of *M. oleifera* concentrations from 19 to 39% and 59%, in the presence of AgNPs have produced broaden inhibition zones, prominently on *S. aureus*. No inhibition zone was observed on the pristine PCL membranes for both bacterial strains, while the addition of AgNPs (PA) and *M. oleifera* leaves extract (PM) alone have demonstrated membrane's antibacterial capability. The statistical analysis depicted that

significant difference existed among the antibacterial electrospun membranes in comparison with the control (PCL) at $p \leq 0.05$ as shown in Fig. 4b.

3.6.2 Bacterial Count Analysis

The PMA-3 electrospun membranes (Fig. 4b) have the highest bactericidal efficacy against *S. aureus* (61.33%) and *E. coli* (28.21%), followed by the PMA-2 and the PMA-1 membranes with more eminent on the *S. aureus* bacterial strain. These records are in accordance with the zone inhibition
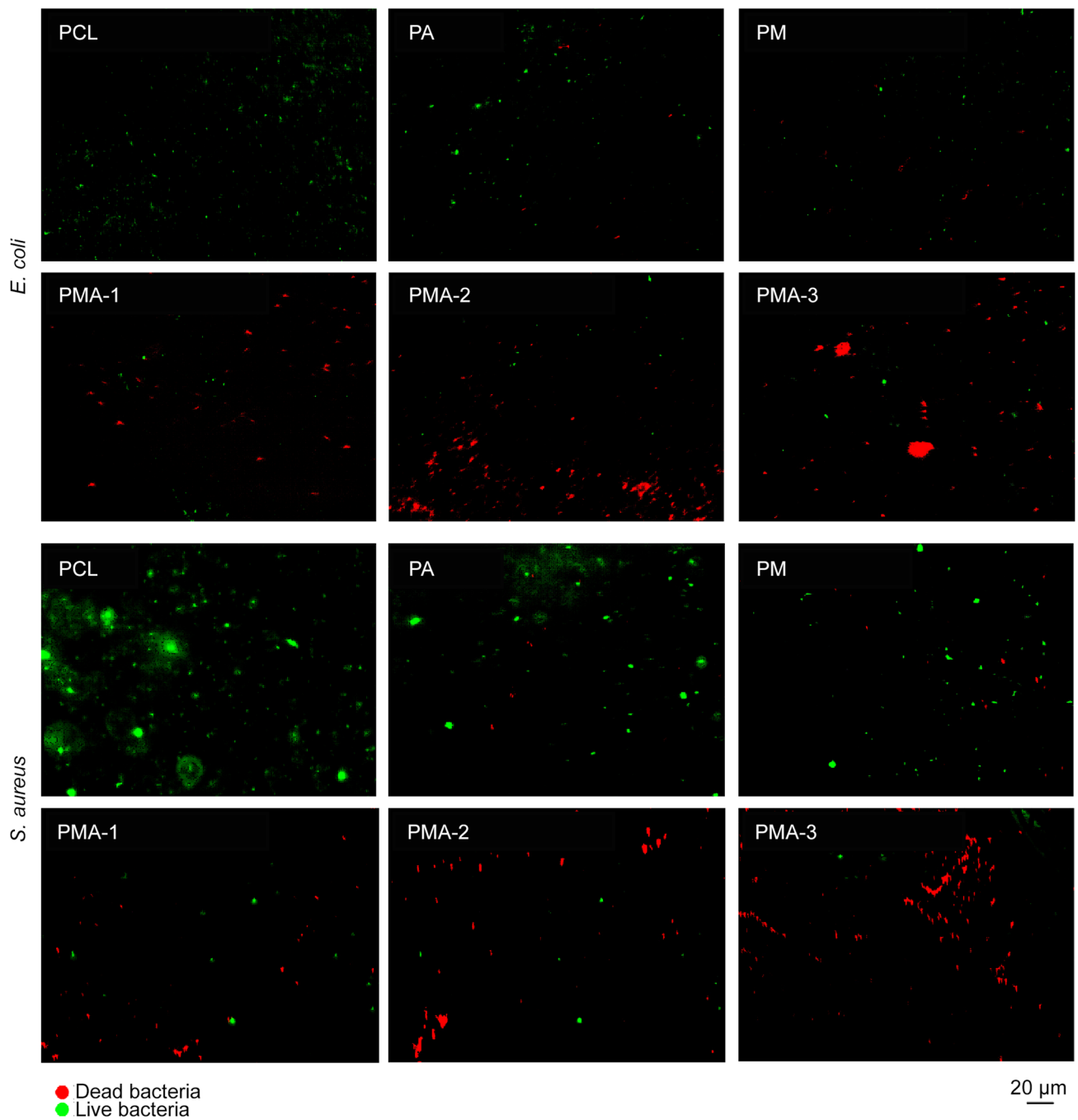
Fig. 5 Stained live/dead bacteria on electrospun PCL, PMA-1, PMA-2 and PMA-3 electrospun membranes after 3 h incubation

results. Two more fabricated electrospun membranes, PA and PM, were also tested to clarify the antibacterial capability of each element, independently. The results pointed out that the membranes blended with only *M. oleifera* leaves extract have shown more efficacy against *S. aureus* in comparison with *E. coli*, while the membranes blended with only AgNPs have displayed more efficacy against *E. coli* than *S. aureus*. However, these results are not identical to the zone inhibition records which might be due to the susceptibility

of bacteria against the used method [26]. For the analysis on *S. aureus*, significant difference was found only on the comparison between the PMA membranes and the control at $p \leq 0.05$. For the analysis on *E. coli*, only the PMA-3 showed significant difference in comparison with the control at $p \leq 0.05$.

The variation in antibacterial effectiveness can be related to the distinct bacterial structures: Gram-positive bacteria's
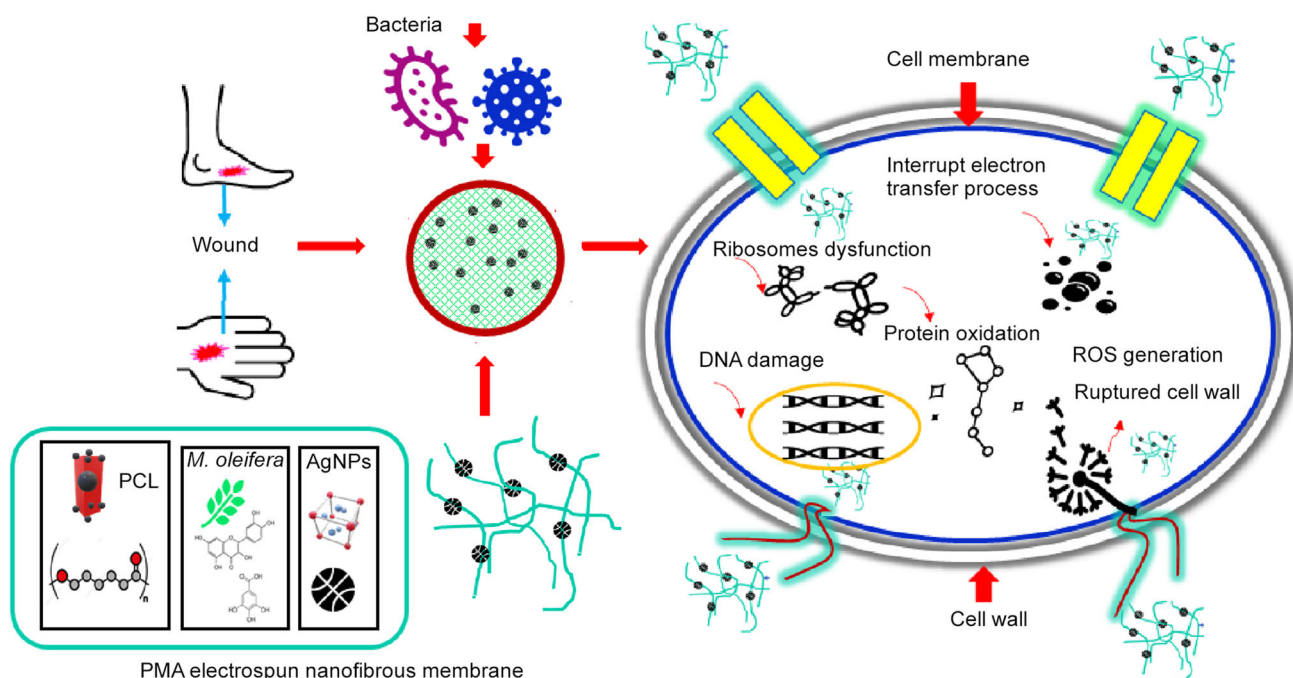
Fig. 6 Antibacterial mechanisms of PMA membranes associated with the action of AgNPs and *M. oleifera* leaves extract

cell wall is a single layer, whereas Gram-negative bacteria's cell wall is a multilayered structure encapsulated by an outer cell membrane [16, 27]. Previous study also demonstrated that aqueous and ethanolic *M. oleifera* leaves extract have stronger antibacterial effect against Gram-positive than Gram-negative bacteria [28]. Recently in the literature, it was reported that AgNPs are inorganic in nature [16], while *M. oleifera* leaves extract is organic in nature [29]. As in our experimental work, only 1% concentration of AgNPs was incorporated into the PCL matrix. Hence, inside the electrospun membranes, organic compounds were dominant. Therefore, it can be concluded that the antibacterial efficacy of the PMA membranes was majorly depended on the concentration of leaves extract which contained various phytochemical compounds.

3.6.3 Live/Dead Staining Analysis

In Fig. 5, the fluorescence images of stained bacteria were captured after 3 h of incubation. This test provides a qualitative measurement that allows the visualization on the fraction of live and dead bacteria on the membranes. As presented in Fig. 5, many live cells were observed on the control (PCL), PA and PM membranes after three hours of incubation, whereas abundance of bacteria was found dead on the PMA-1, PMA-2 and PMA-3 membranes. This trend was in accordance with the results of zone inhibition and bacterial count analyses.

The PMA electrospun membranes have released phytochemical compounds along with the Ag ions to kill bacteria in the liquid media and destroyed them by damaging their cell membranes and intracellular metabolisms [30, 31]. Figure 6 presents the antibacterial mechanisms, associated with the antibacterial effects of PMA membranes. The interaction between the PMA electrospun membranes and the bacterial cell was facilitated by the negatively charged cell membranes. The positive Ag ions [16] and the *M. oleifera* phytochemicals, especially Quercetin, [8] were in contact with the bacterial walls, caused changes in the membrane structure and function which allowed the penetration of both elements through the ruptured cell membranes. The Ag ions and the *M. oleifera* phytochemicals further interrupted the bacterial metabolic processes including the protein deactivation and the nucleus modification that involved DNA and ribosome damages. There are some evidences stated that *M. oleifera* leaves extract and AgNPs may generate reactive oxygen such as peroxides, oxygen radicals and hydroxyl radicals [32, 33]. Further comparison is required to corroborate this idea.

3.7 Hemocompatibility Measurement

3.7.1 Anticoagulant Analysis

In physiological circumstances, biomaterials are effectively surrounded by plasma protein and platelet, which quickly attach to the biomaterial surface and accelerated a cascade of blood clot formation. The time required for clotting event
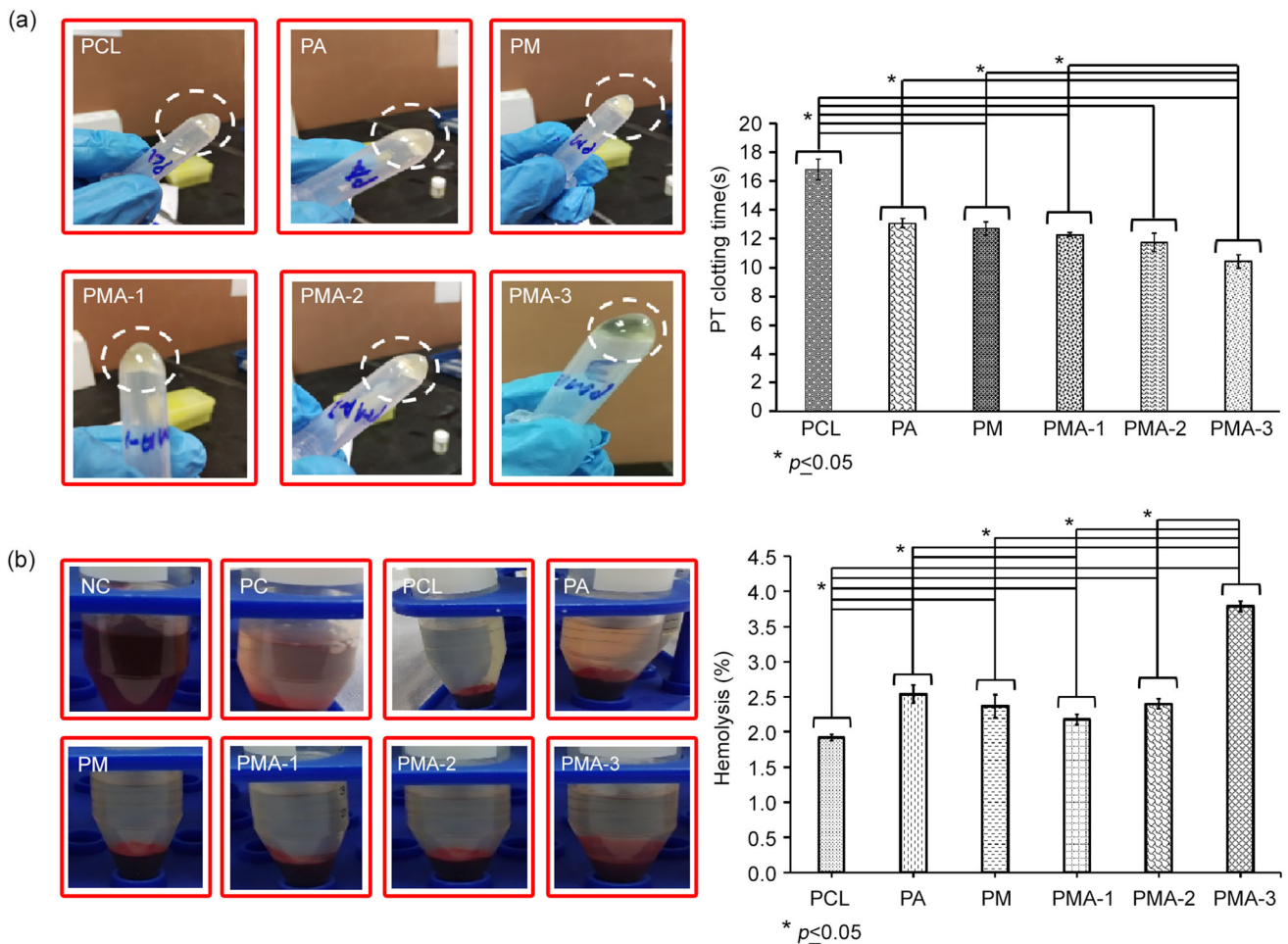
Fig. 7 **a** Blood compatibility PT and **b** hemolysis analyses on electrospun membranes: Blood responses and graphical data representation ($p \leq 0.05$)

Table 2 TGA and DTG results of PCL, PMA-1, PMA-2 and PMA-3 electrospun membranes

Parameter	PCL	PMA-1	PMA-2	PMA-3
Initial onset temperature (°C)	380	230	200	200
Quasistatic temperature (°C)	400–430	410–430	420–430	425–430
ΔWeight decomposition (%)	99.96	94.35	90.45	84.24
Residue (%)	3	4	11	22
T_{max} (°C)	383.76	395.52	400.52	395.22
Derivative weight (%/min)	− 45	− 18	− 15	− 11

may be affected by the surface quality of biomaterials or the presence of bioactive substances [34]. In this study, a decrease in clotting time was notified as shown in Fig. 7a. The electrospun membranes contained Ag and *M. oleifera* leaves extract showed less clotting time significantly within the range of theoretical period (PT 10–15 s) [35], in comparison with the PCL electrospun membranes. However, increasing the concentration of *M. oleifera* did not produce significant decrement in clotting time when compared among the PMA membranes except for the PMA-3. The PMA-3 able to reduce

the clotting time 39% compared to the PCL electrospun membranes.

The nanofibrous electrospun membranes loaded with bioactive agents can give an interesting alternative in wound healing formulation due to their ability to support hemostasis [36]. It was reported that the main criteria to activate the coagulation cascade are platelet adhesion and aggregation. Platelet factors released by active platelets can activate prothrombin, leading to coagulation [36]. Moreover, fiber diameter, increase in hydrophilicity, surface roughness and

pore size also play important roles to enhance the coagulant activity of electrospun membranes.

3.7.2 Hemolysis Analysis

Hemolysis happens when cells enlarge to a critical mass, causing the cell membranes to rupture. It is crucial to assess the hemolysis index in testifying the hemocompatibility of electrospun membranes [37]. The cytotoxicity of the electrospun membranes towards human blood requires clarification as the membranes will be in contact with the blood during the membrane placement. A significant difference ($p \leq 0.05$) was notated between all electrospun membranes compared to the 100% hemolysis negative control, PCL and PMA-3, respectively (Fig. 7b). Even though the incorporation of *M. oleifera* and Ag into the PCL membranes increased the hemolysis index, all fabricated membranes were within the standard range of hemocompatible material which is $\leq 5\%$ [38, 39].

The agglomerated Ag compounds were viewed in the PMA-2 and PMA-3 membranes which may induce cellular stress and production of oxidative stress which can damage biological entities [40, 41]. Besides, *M. oleifera* is composed of polar solvent in the form of phytochemical compounds, allowing the polar content to cross over cell membrane, change the hypertonic state and exert pressure on the red blood cells to swell/rupture [29]. However, the effects of hemolysis are not dominant on the PMA electrospun membranes with the record of $\leq 5\%$ hemolysis index and therefore, safe to be used as tissue membrane for wound healing.

4 Conclusion

In this study, *M. oleifera* leaves extract was blended into PCL/AgNPs electrospun membranes using an electrospinning method. The characterization analyses demonstrated that the nanofiber diameter, pore size, hydrophilicity, surface roughness and thermal stability were depended on the concentrations of *M. oleifera* leaves extract where the change in the *M. oleifera* concentration will subsequently alter the PCL concentration at the standard 1 wt% Ag composition. The fingerprints of *M. oleifera* were observed through the appearances of C=C and N–O functional groups, while the Ag composition was recorded to be less than 1 wt% for all PMA membranes. The PMA membranes were more susceptible in killing Gram-positive *S. aureus* than Gram-negative *E. coli* through the release of antibacterial agents and the antibacterial action mechanism. The presence of methanolic extract of *M. oleifera* and AgNPs has improved the platelet coagulant behavior of the PCL membranes where these membranes were classified as hemocompatible materials.

References

1. Shin, J.U.; Gwon, J.; Lee, S.-Y.; Yoo, H.S.: Silver-incorporated nanocellulose fibers for antibacterial hydrogels. ACS Omega **3**, 16150–16157 (2018). https://doi.org/10.1021/acsomega.8b02180
2. Liu, R.; Dai, L.; Si, C.; Zeng, Z.: Antibacterial and hemostatic hydrogel via nanocomposite from cellulose nanofibers. Carbohydr. Polym. **195**, 63–70 (2018). https://doi.org/10.1016/j.carbpol.2018.04.085
3. Laurano, R.; Boffito, M.; Ciardelli, G.; Chiono, V.: Wound dressing products: a translational investigation from the bench to the market. Eng. Regen. **3**, 182–200 (2022). https://doi.org/10.1016/j.engreg.2022.04.002
4. Yousefi, I.; Pakravan, M.; Rahimi, H.; Bahador, A.; Farshadzadeh, Z.; Haririan, I.: An investigation of electrospun henna leaves extract-loaded chitosan based nanofibrous mats for skin tissue engineering. Mater. Sci. Eng. C **75**, 433–444 (2017). https://doi.org/10.1016/j.msec.2017.02.076
5. Doustdar, F.; Ramezani, S.; Ghorbani, M.; Moghadam, F.M.: Optimization and characterization of a novel tea tree oil-integrated poly(ε-caprolactone)/soy protein isolate electrospun mat as a wound care system. Int. J. Pharm. **627**, 122218 (2022). https://doi.org/10.1016/j.ijpharm.2022.122218
6. Almasian, A.; Najafi, F.; Eftekhari, M.; Ardekani, M.R.S.; Sharifzadeh, M.; Khanavi, M.: Polyurethane/carboxymethylcellulose nanofibers containing Malva sylvestris extract for healing diabetic wounds: preparation, characterization, in vitro and in vivo studies. Mater. Sci. Eng. C **114**, 111039 (2020). https://doi.org/10.1016/j.msec.2020.111039
7. Muhammad, A.A.; Arulselvan, P.; Cheah, P.S.; Abas, F.; Fakurazi, S.: Evaluation of wound healing properties of bioactive aqueous fraction from Moringa oleifera Lam on experimentally induced diabetic animal model. Drug Des. Dev. Ther. **10**, 1715 (2016). https://doi.org/10.2147/DDDT.S96968
8. Bagheri, G.; Martorell, M.; Ramirez, A.K.; Salehi, B.; Sharifi, R.J.: Phytochemical screening of *Moringa oleifera* leaf extracts and their antimicrobial activities. Cell. Mol. Biol. **1**, 20–26 (2020). https://doi.org/10.14715/cmb/2019.66.1.3
9. Mahato, D.K.; Kargwal, R.; Kamle, M.; Sharma, B.; Pandhi, S.; Mishra, S.; Gupta, A.; Chayan Mahmud, M.M.; Gupta, M.K.; Singha, L.B.; Kumar, P.: Ethnopharmacological properties and nutraceutical potential of *Moringa oleifera*. Phytomed. Plus. **2**, 100168 (2022). https://doi.org/10.1016/j.phyplu.2021.100168
10. Fahimirad, S.; Abtahi, H.; Satei, P.; Ghaznavi, R.E.; Moslehi, M.; Ganji, A.: Wound healing performance of PCL/chitosan based electrospun nanofiber electrosprayed with curcumin loaded chitosan nanoparticles. Carbohydr. Polym. **259**, 117640 (2021). https://doi.org/10.1016/j.carbpol.2021.117640
11. Malikmammadov, E.; Tanir, T.E.; Kiziltay, A.; Hasirci, V.; Hasirci, N.: PCL and PCL-based materials in biomedical applications. J. Biomater. Sci. **29**, 7–9 (2017). https://doi.org/10.1080/09205063.2017.1394711
12. Ji, X.; Li, R.; Liu, G.; Jia, W.; Sun, M.; Liu, Y.; Luo, Y.; Cheng, Z.: Phase separation-based electrospun janus nanofibers loaded with *Rana chensinensis* skin peptides/silver nanoparticles for wound

healing. Mater. Des. **207**, 109864 (2021). https://doi.org/10.1016/j.matdes.2021.109864

13. Iacob, A.T.; Dragan, M.; Ionescu, O.M.; Profire, L.; Ficai, A.; Andronescu, E.; Georgeta, L.; Lupascu, D.: An overview of biopolymeric electrospun nanofibers based on polysaccharides for wound healing management. Pharmaceutics **12**, 10 (2020). https://doi.org/10.3390/pharmaceutics12100983

14. Chin, C.-Y.; Ng, S.-F.: Development of *Moringa oleifera* standardized leaf extract nanofibers incorporated onto hydrocolloid film as a potential chronic wound dressing. Fibers Polym. **11**, 2462–2472 (2020). https://doi.org/10.1007/s12221-020-1356-9

15. Augustine, R.; Malik, H.N.; Singhal, D.K.; Mukherjee, A.; Malakar, D.; Kalarikkal, N.; Thomas, S.: Electrospun polycaprolactone/ZnO nanocomposite membranes as biomaterials with antibacterial and cell adhesion properties. J. Polym. Res. **3**, 1–17 (2014). https://doi.org/10.1007/s10965-013-0347-6

16. Saidin, S.; Jumat, M.A.; Amin, N.; Al-Hammadi, A.S.S.: Organic and inorganic antibacterial approaches in combating bacterial infection for biomedical application. Mater. Sci. Eng. C **118**, 111382 (2021). https://doi.org/10.1016/j.msec.2020.111382

17. Du, L.; Xu, H.; Li, T.; Zhang, Y.; Zou, F.: Fabrication of silver nanoparticle/polyvinyl alcohol/polycaprolactone hybrid nanofibers nonwovens by two-nozzle electrospinning for wound dressing. Fibers Polym. **12**, 1995–2005 (2016). https://doi.org/10.1007/s12221-016-6813-0

18. He, C.; Liu, X.; Zhou, Z.; Liu, N.; Ning, X.; Miao, Y.; Long, Y.; Wu, T.; Leng, X.: Harnessing biocompatible nanofibers and silver nanoparticles for wound healing: sandwich wound dressing versus commercial silver sulfadiazine dressing. Mater. Sci. Eng. C **128**, 112342 (2021). https://doi.org/10.1016/j.msec.2021.112342

19. Daud, N.M.; Masri, N.A.N.; Nik Malek, N.A.; Razak, S.I.A.; Saidin, S.: Long-term antibacterial and stable chlorhexidine-polydopamine coating on stainless steel 316L. Prog. Org. Coat. **122**, 147–153 (2018). https://doi.org/10.1016/j.porgcoat.2018.05.012

20. Jaganathan, S.K.; Mani, M.P.: Electrospinning synthesis and assessment of physicochemical properties and biocompatibility of cobalt nitrate fibers for wound healing applications. An. Acad. Bras. Cienc. (2019). https://doi.org/10.1590/0001-3765201920180237

21. Ravichandran, S.; Radhakrishnan, J.; Jayabal, P.; Venkatasubbu, G.D.: Antibacterial screening studies of electrospun polycaprolactone nano fibrous mat containing *Clerodendrum phlomidis* leaves extract. Appl. Surf. Sci. **484**, 676–687 (2019). https://doi.org/10.1016/j.apsusc.2019.04.150

22. Sun, J.; Wanga, Q.; Luo, G.; Menga, W.; Cao, M.; Li, Y.; Masterman-Smithc, M.D.; Yanga, H.; Sun, X.; Lang, M.-F.: A novel flexible Ag/AgCl quasi-reference electrode based on silver nanowires toward ultracomfortable electrophysiology and sensitive electrochemical glucose detection. J. Mater. Res. Technol. **9**, 13425–13433 (2020). https://doi.org/10.1016/j.jmrt.2020.09.041

23. Goonoo, N.; Bhaw, L.A.; Rodriguez, I.A.; Wesner, D.; Schönherr, H.; Bowlin, G.L.; Jhurry, D.: Poly(ester-ether) s: III. Assessment of cell behaviour on nanofibrous scaffolds of PCL, PLLA and PDX blended with amorphous PMeDX. J. Mater. Chem. B **4**, 673–687 (2015). https://doi.org/10.1039/C4TB01350F

24. Brilhante, R.S.N.; Sales, J.A.; Pereira, V.S.; de Souza Collares MaiaCastelo Branco, D.; de Aguiar Cordeiro, R.; de Souza Sampaio, C.M.; de Araújo Neto Paiva, M.; dos Santos, J.B.F.; Sidrim, J.J.C.; Rocha, M.F.G.: Research advances on the multiple uses of *Moringa oleifera*: a sustainable alternative for socially neglected population. Asian Pac. J. Trop. Med. **7**, 621–630 (2017). https://doi.org/10.1016/j.apjtm.2017.07.002

25. Ramalingam, R.; Dhand, C.; Leung, C.M.; Ezhilarasu, H.; Prasannan, P.; Ong, S.T.; Subramanian, S.; Kamruddin, M.; Lakshminarayanan, R.; Ramakrishna, S.: Poly-ε-caprolactone/gelatin hybrid electrospun composite nanofibrous mats containing ultrasound assisted herbal extract: antimicrobial and cell proliferation study. Nanomaterials **3**, 462 (2019). https://doi.org/10.3390/nano9030462

26. Haase, H.; Jordan, L.; Keitel, L.; Keil, C.; Mahltig, B.: Comparison of methods for determining the effectiveness of antibacterial functionalized textiles. PLoS ONE **11**, e0188304 (2017). https://doi.org/10.1371/journal.pone.0188304

27. Gothai, S.; Arulselvan, P.; Tan, W.S.; Fakurazi, S.: Wound healing properties of ethyl acetate fraction of *Moringa oleifera* in normal human dermal fibroblasts. J. Intercult. Ethnopharmacol. (2016). https://doi.org/10.5455/jice.20160201055629

28. Abd, R.N.Z.; Husain, K.; Kumolosasi, E.: *Moringa* genus: a review of phytochemistry and pharmacology. Front. Pharmacol. **9**, 26 (2018). https://doi.org/10.3389/fphar.2018.00108

29. Jiang, M.Y.; Lu, H.; Pu, X.Y.; Li, Y.H.; Tian, K.; Xiong, Y.; Wang, W.; Huang, X.Z.: Laxative metabolites from the leaves of Moringa oleifera. J. Agric. Food Chem. **30**, 7850–7860 (2020). https://doi.org/10.1021/acs.jafc.0c01564

30. Augustine, R.; Kalarikkal, N.; Thomas, S.: Electrospun PCL membranes incorporated with biosynthesized silver nanoparticles as antibacterial wound dressings. Appl. Nanosci. **3**, 337–344 (2016). https://doi.org/10.1007/s13204-015-0439-1

31. Fayemi, O.E.; Ekennia, A.C.; Katata-Seru, L.; Ebokaiwe, A.P.; Ijomone, O.M.; Onwudiwe, D.C.; Ebenso, E.E.: Antimicrobial and wound healing properties of polyacrylonitrile-*Moringa* extract nanofibers. ACS Omega **5**, 4791–4797 (2018). https://doi.org/10.1021/acsomega.7b01981

32. Hashim, F.J.; Vichitphan, S.; Boonsiri, P.; Vichitphan, K.: Neuroprotective assessment of *Moringa oleifera* leaves extract against oxidative-stress-induced cytotoxicity in SHSY5Y neuroblastoma cells. Plants **5**, 14 (2021). https://doi.org/10.3390/plants10050889

33. Jatoi, A.W.; Kim, I.S.; Ogasawara, H.; Ni, Q.Q.: Characterizations and application of CA/ZnO/AgNP composite nanofibers for sustained antibacterial properties. Mater. Sci. Eng. C **105**, 8 (2019). https://doi.org/10.1016/j.msec.2019.110077

34. Teixeira, M.A.; Antunes, J.C.; Seabra, C.L.; Tohidi, S.D.; Reis, S.; Amorim, M.T.P.; Felgueiras, H.P.: Tiger 17 and Pexiganan as antimicrobial and hemostatic boosters of cellulose acetate-containing poly(vinyl alcohol) electrospun mats for potential wound care purposes. Int. J. Biol. Macromol. **209**, 1526–1541 (2022). https://doi.org/10.1016/j.bioadv.2022.212830

35. Horakova, J.; Oulehlova, Z.; Novotny, V.; Jencova, V.; Mikes, P.; Havlickova, K.; Prochazkova, R.; Heczkova, B.; Hadinec, P.; Sehr, S.: The assessment of electrospun scaffolds fabricated from polycaprolactone with the addition of L-arginine. Biomed. Phys. Eng. Express **2**, 025012 (2020)

36. Horakova, J.; Mikes, P.; Saman, A.; Svarcova, T.; Jencova, V.; Suchy, T.; Heczkova, B.; Jakubkova, S.; Jirousova, J.; Prochazkova, R.: Comprehensive assessment of electrospun scaffolds hemocompatibility. Mater. Sci. Eng. C **82**, 330–335 (2018). https://doi.org/10.1016/j.msec.2017.05.011

37. Singhal, J.P.; Ray, A.R.: Synthesis of blood compatible polyamide block copolymers. Biomaterials **4**, 1139–1145 (2002). https://doi.org/10.1016/S0142-9612(01)00228-9

38. Abdollahi, S.; Raoufi, Z.: Gelatin/Persian gum/bacterial nanocellulose composite films containing frankincense essential oil and Teucrium polium extract as a novel and bactericidal wound dressing. Drug Deliv. Sci. Technol. **72**, 103423 (2022). https://doi.org/10.1016/j.jddst.2022.103423

39. Alippilakkotte, S.; Kumar, S.; Sreejith, L.: Fabrication of PLA/Ag nanofibers by green synthesis method using Momordica charantia fruit extract for wound dressing applications. Colloids Surf. A Physicochem. Eng. Asp. **529**, 771–782 (2017). https://doi.org/10.1016/j.colsurfa.2017.06.066

40. Kalantari, K.; Mostafavi, E.; Afifi, A.M.; Izadiyan, Z.; Jahangirian, H.; Rafiee, M.R.; Webster, T.J.: Wound dressings functionalized with silver nanoparticles promises and pitfalls. Nanoscale **4**, 2268–2291 (2020). https://doi.org/10.1039/C9NR08234D

41. Kim, S.; Ryu, D.Y.J.: Silver nanoparticle-induced oxidative stress, genotoxicity and apoptosis in cultured cells and animal tissues. Appl. Toxicol. **2**, 78–89 (2013). https://doi.org/10.1002/jat.2792